



# Allergologia et immunopathologia

Sociedad Española de Inmunología Clínica,  
Alergología y Asma Pediátrica

[www.all-imm.com](http://www.all-imm.com)



ORIGINAL ARTICLE

OPEN ACCESS

## Knockdown of EPSTI1 alleviates lipopolysaccharide-induced inflammatory injury through regulation of NF- $\kappa$ B signaling in a cellular pneumonia model

Adilijiang Kari, Zhihua M, Zhayidan Aili, Ayinuerguli Adili, Nadire Hairula, Abulaiti Abuduhaer\*

*Pediatric Intensive Care Unit, First Affiliated Hospital of Xinjiang Medical University, Urumqi, China*

Received 12 January 2022; Accepted 21 February 2022

Available online 1 May 2022

### KEYWORDS

epithelial-stromal interaction 1; inflammation; nuclear factor  $\kappa$ -light-chain-enhancer of activated B cells; pneumonia

### Abstract

**Background:** Although early diagnosis, antibiotic therapies, corticosteroid application, and health care services are conventional managements for pneumonia, antibiotic resistance and adverse reactions remain as limitations for pneumonia treatment.

**Objectives:** The study attempted to evaluate the potential role of EPSTI1 against pneumonia and reveal its underlying mechanism.

**Methods:** Lipopolysaccharide (LPS) (5, 10, and 20  $\mu$ g/mL) was applied in WI-38 cells to establish the *in vitro* pneumonia model. Knockdown of epithelial-stromal interaction 1 (EPSTI1) was performed by transfection with EPSTI1 siRNA (siEPSTI1) into LPS-treated cells. Cell Counting Kit-8 assays were implemented to measure cell viability, and apoptotic cells were detected using flow cytometry. Interleukin-1 $\beta$  (IL-1 $\beta$ ), IL-6, and tumor necrosis factor- $\alpha$  (TNF- $\alpha$ ) were quantified using enzyme-linked immunosorbent assay (ELISA). Immunoblotting and quantitative real-time polymerase chain reaction (qRT-PCR) were conducted to quantify EPSTI1 expression, and proteins related to nuclear factor  $\kappa$ -light-chain-enhancer of activated B cell (NF- $\kappa$ B) signaling, including p-p65, p65, p-I $\kappa$ B $\alpha$ , and I $\kappa$ B $\alpha$ .

**Results:** EPSTI1 was highly expressed in LPS-treated WI-38 cells. Cell apoptosis was promoted, and cell viability was inhibited after being exposed to LPS. Besides, IL-1 $\beta$ , IL-6, and TNF- $\alpha$  were dramatically upregulated. Knockdown of EPSTI1 restored cell viability, inhibited cell apoptosis, and attenuated expressions of proinflammatory factors. Additionally, knockdown of EPSTI1 visibly decreased the increased ratios of p-p65/p65 and p-I $\kappa$ B $\alpha$ /I $\kappa$ B $\alpha$  induced by LPS. Knockdown of EPSTI1 alleviated inflammatory injury through the inactivation of the NF- $\kappa$ B pathway.

**Conclusions:** These results provided promising management in preventing pneumonia in patients.

© 2022 Codon Publications. Published by Codon Publications.

\*Corresponding author: Abulaiti-Abuduhaer, Pediatric Intensive Care Unit, First Affiliated Hospital of Xinjiang Medical University, No. 137 Liyushan South Road, Xinshi District, Urumqi, Xinjiang 830054, China. Email address: [abulati1077@163.com](mailto:abulati1077@163.com)

<https://doi.org/10.15586/aei.v50i3.581>

Copyright: Kari A, et al.

License: This open access article is licensed under Creative Commons Attribution 4.0 International (CC BY 4.0). <http://creativecommons.org/>

## Introduction

Pneumonia is a lower respiratory tract disease infected by pathogens and manifested as inflammatory responses.<sup>1</sup> The overall mortality of pneumonia was 2.9%-8.0% in China depending on different regions.<sup>2</sup> Early diagnosis, appropriate antibiotic therapies, and the use of corticosteroids and health care services remain as conventional managements for pneumonia.<sup>1,3</sup> However, due to antibiotic resistance and adverse reactions, the optimal management of pneumonia is a 'hot topic'.

Epithelial-stromal interaction 1 (EPSTI1), a gene mapped to human chromosome 13q13.3, was first discovered as a stromal fibroblast gene in breast cancer.<sup>4</sup> Previous studies have demonstrated that EPSTI1 plays pivotal roles in ovarian tumorigenesis,<sup>5</sup> lung squamous cell cancers,<sup>6</sup> and prostate cancer development.<sup>7</sup> Besides, EPSTI1 expression is remarkably elevated in alveolar epithelial type II cells from COPD patients.<sup>8</sup> Recently, EPSTI1 was highly expressed in peripheral blood and bronchoalveolar lavage fluid of patients with COVID-19.<sup>9</sup> EPSTI1 is implicated in diseases related to inflammatory signaling,<sup>10</sup> and excessive EPSTI1 induces the hyperactivation of B cell by regulating NF- $\kappa$ B signaling in primary Sjögren's syndrome.<sup>11</sup> Unfortunately, the involvement of EPSTI1 in pneumonia remains unclear.

The inflammatory response is certainly related to acute and chronic diseases, and NF- $\kappa$ B is essential not only in the proinflammatory phase but also in the stage of anti-inflammatory gene expression and inducing apoptosis.<sup>12</sup> Oxidative stress and the NF- $\kappa$ B pathway participate in the development of influenzal pneumonia, while inactivation of the NF- $\kappa$ B pathway could attenuate the replication of influenza A virus.<sup>13</sup> In children with pneumonia, inhibition of the NF- $\kappa$ B pathway alleviates the inflammatory responses.<sup>14</sup> This study attempted to investigate whether EPSTI1 was involved in pneumonia through regulating the NF- $\kappa$ B pathway. Therefore, lipopolysaccharide (LPS) was applied to establish a cellular pneumonia model in WI-38 cells, and knockdown of EPSTI1 was subsequently performed, followed by determining the involvement of NF- $\kappa$ B signaling.

## Methods

### *Cell culture and in vitro pneumonia model induction*

Human fetal lung fibroblast WI-38 cells obtained from the American Type Culture Collection (ATCC; Rockville, Maryland, USA) were maintained in a DMEM medium (Gibco, Grand Island, NY, USA), supplemented with 10% fetal bovine serum, 100  $\mu$ g/mL streptomycin, and 100 U/mL penicillin (Invitrogen, Carlsbad, CA, USA) at 37°C with 5% CO<sub>2</sub>. When cells were grown to 80% confluence, WI-38 cells at a density of 2 $\times$ 10<sup>5</sup> cells/well were placed in six-well plates and cultured for 48 h at 37°C. Afterward, LPS (5, 10, and 20  $\mu$ g/mL) was applied to WI-38 cells and then incubated for 24 h.

### *SiRNA transfection*

For knockdown of EPSTI1, EPSTI1 siRNA and a negative control (siNC) were bought from GenePharma (Shanghai,

China), which were subsequently transfected into WI-38 cells using Lipofectamine 2000 (Invitrogen, Carlsbad, CA, USA) according to the manufacturer's instructions. After 48 h of transfection, cells were harvested for further experiments.

### *Cell viability*

WI-38 cells (5 $\times$ 10<sup>3</sup> cells/well) were placed in 96-well plates. After 24 h of LPS stimuli or 48 h of siEPSTI1 transfection, cell viability was assessed using a CCK-8 assay kit (Beyotime Biotechnology, Jiangsu Province, China) according to the manufacturer's instructions. The optical density was read at 450 nm using a microplate reader (Thermo Scientific, San Jose, CA, USA).

### *Cell apoptosis*

Cells were collected after 48 h of transfection, rinsed with PBS, and then resuspended using 100  $\mu$ L of buffer. Subsequently, 10  $\mu$ L of Annexin V-FITC was applied to cells in the dark for 30 min, followed by addition of 5  $\mu$ L of propidium iodide for 15 min. Cell apoptosis was detected using FACScan flow cytometry (Becton Dickinson, Franklin Lakes, NJ, USA).

### *ELISA*

Cells (1 $\times$ 10<sup>5</sup> cells/well) were placed in 24-well plates for 24 h, and the culture supernatant was obtained. The levels of IL-6 (ab178013, Abcam, Cambridge, MA, USA), IL-18 (ab214025, Abcam, Cambridge, MA, USA), and TNF- $\alpha$  (ab181421, Abcam, Cambridge, MA, USA) were determined using ELISA kits according to the manufacturer's instructions (Invitrogen, Carlsbad, CA, USA).

### *RT-qPCR*

For total RNA extraction, TRIzol reagent (LanGang biological, China) was implemented in LPS-treated or siEPSTI1-transfected WI-38 cells. First-strand cDNA was synthesized using a SuperScript III Reverse Transcriptase kit (Invitrogen, Carlsbad, CA, USA). Next, qRT-PCR was conducted using a SYBR® Premix Ex Taq™ II kit (TaKaRa, Japan) on an ABI 7300 real-time PCR detection system (Applied Biosystems, Foster City, CA, USA) at 95°C for 5 min, followed by 40 cycles at 94°C for 30 s, 56°C for 90 s, and 72°C for 60 s. The primers for EPSTI1 were 5'-ACCCGCAATAGAGTGGTGAAC-3' (forward) and 5'-GCTATCAAGGTGTATGCACTTGT-3' (reverse). The gene expression was quantified using the 2<sup>- $\Delta\Delta$ Ct</sup> method.<sup>15</sup>

### *Immunoblotting analysis*

Total proteins were obtained from LPS-treated or siEPSTI1-transfected WI-38 cells by RIPA lysis buffer. Proteins were electrophoresed on 10% SDS-PAGE, transferred onto poly(vinylidene difluoride) membranes, and then blocked with 5%

nonfat milk, followed by incubation with antibodies against EPST11 (1:200, sc-100657, Santa Cruz, CA, USA), B-cell lymphoma-2 (Bcl-2, 1:100, sc-166943, Santa Cruz, CA, USA), Bcl-2 associated x protein (Bax, 1:200, sc-7480, Santa Cruz), cleaved-caspase 3 (1:500, ab32042, Abcam), cleaved-caspase 9 (1:500, ab2324, Abcam), p-p65 (1:500, ab31624, Abcam), p65 (1:1000, ab32536, Abcam), p-IkBa (1:200, sc-8404, Santa Cruz), and IkBa (1:200, sc-1643, Santa Cruz) at 4°C overnight. Afterward, membranes were incubated with peroxidase-conjugated goat anti-rabbit IgG antibodies (1:2000, ab205718, Abcam) for 2 h. Blots were visualized with an enhanced chemiluminescence kit (Millipore, Billerica, MA, USA).

### Statistical analysis

Data were analyzed using SPSS 17.0 software (Chicago, IL, USA) and exhibited as mean  $\pm$  SD. ANOVA was applied for comparison between multiple groups, followed by Tukey's post hoc tests. The value of  $p$  was set to 0.05.

## Results

### EPST11 was highly expressed in LPS-treated WI-38 cells

After being exposed to LPS, the expression of EPST11 in WI-38 cells was quantified using RT-qPCR and immunoblotting. As presented in Figure 1A,B, 10  $\mu$ g/mL and 20  $\mu$ g/mL LPS dramatically promoted EPST11 expression in WI-38 cells ( $P < 0.01$  or 0.001). LPS stimuli remarkably inhibited the viability of WI-38 cells in a dose-dependent manner. Collectively, EPST11 was downregulated by LPS stimuli in a dose-dependent manner.

### Knockdown of EPST11 repressed the apoptosis of LPS-treated WI-38 cells

To investigate whether EPST11 was implicated in the inhibitory effect of LPS (10  $\mu$ g/mL) on cell survival, siEPST11 was subsequently transfected into LPS-treated WI-38 cells. Figure 2A,B displays that LPS induced a significant increase in EPST11 expression compared to the control ( $P < 0.001$ ), while siEPST11 remarkably suppressed the level of EPST11 compared to siNC ( $P < 0.01$ ). After treatment of LPS for 24h, the viability of WI-38 cells was significantly inhibited compared to that of the control ( $P < 0.001$ ), which was dramatically increased after siEPST11 transfection ( $P < 0.05$ ) (Figure 2C). LPS also caused a higher apoptotic rate of WI-38 cells than the control ( $P < 0.001$ ), while siEPST11 suppressed the LPS-induced apoptotic rate compared to that of transfection of siNC ( $P < 0.001$ ) (Figure 2D). Besides, immunoblotting portrayed that Bax, cleaved caspase 3, or cleaved caspase 9 were significantly upregulated, but Bcl-2 was downregulated after LPS treatment compared with those of the control ( $P < 0.001$ ). However, transfection with siEPST11 reversed these results (Figure 2D). Taken together, knockdown of EPST11 repressed the apoptosis of LPS-treated WI-38 cells.

### Knockdown of EPST11 suppressed inflammatory responses in LPS-treated WI-38 cells

Subsequently, the levels of IL-6, IL-1B, and TNF- $\alpha$  were determined by ELISA, and Figure 3A shows that 10  $\mu$ g/mL LPS induced distinct increases in IL-6, IL-8, and TNF- $\alpha$  as compared to those of the control ( $P < 0.001$ ), whereas siEPST11 remarkably suppressed these inflammatory cytokines as compared to those of siNC ( $P < 0.01$  or 0.05).

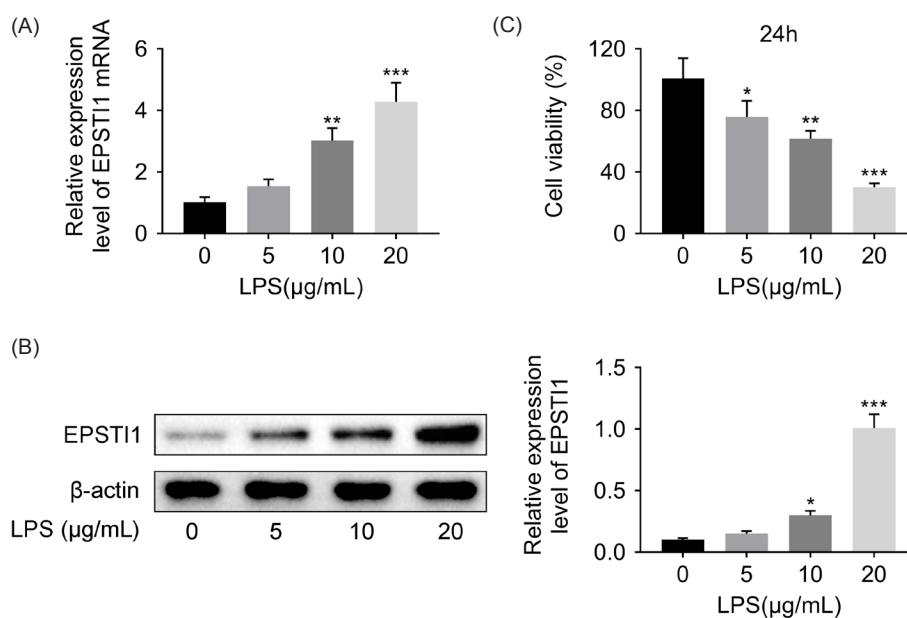


**Figure 1** EPST11 was highly expressed in LPS-treated WI-38 cells. (A) EPST11 expression was quantified by RT-qPCR after different concentrations of LPS (5, 10, 20  $\mu$ g/mL) in WI-38 cells. (B) Protein level of EPST11 was determined by western blot analysis when stimulated by LPS in WI-38 cells. (C) Viability of LPS-treated WI-38 cells was assessed using CCK-8 assay. \* $P < 0.05$ , \*\* $P < 0.01$ , and \*\*\* $P < 0.001$  versus untreated WI-38 cells.

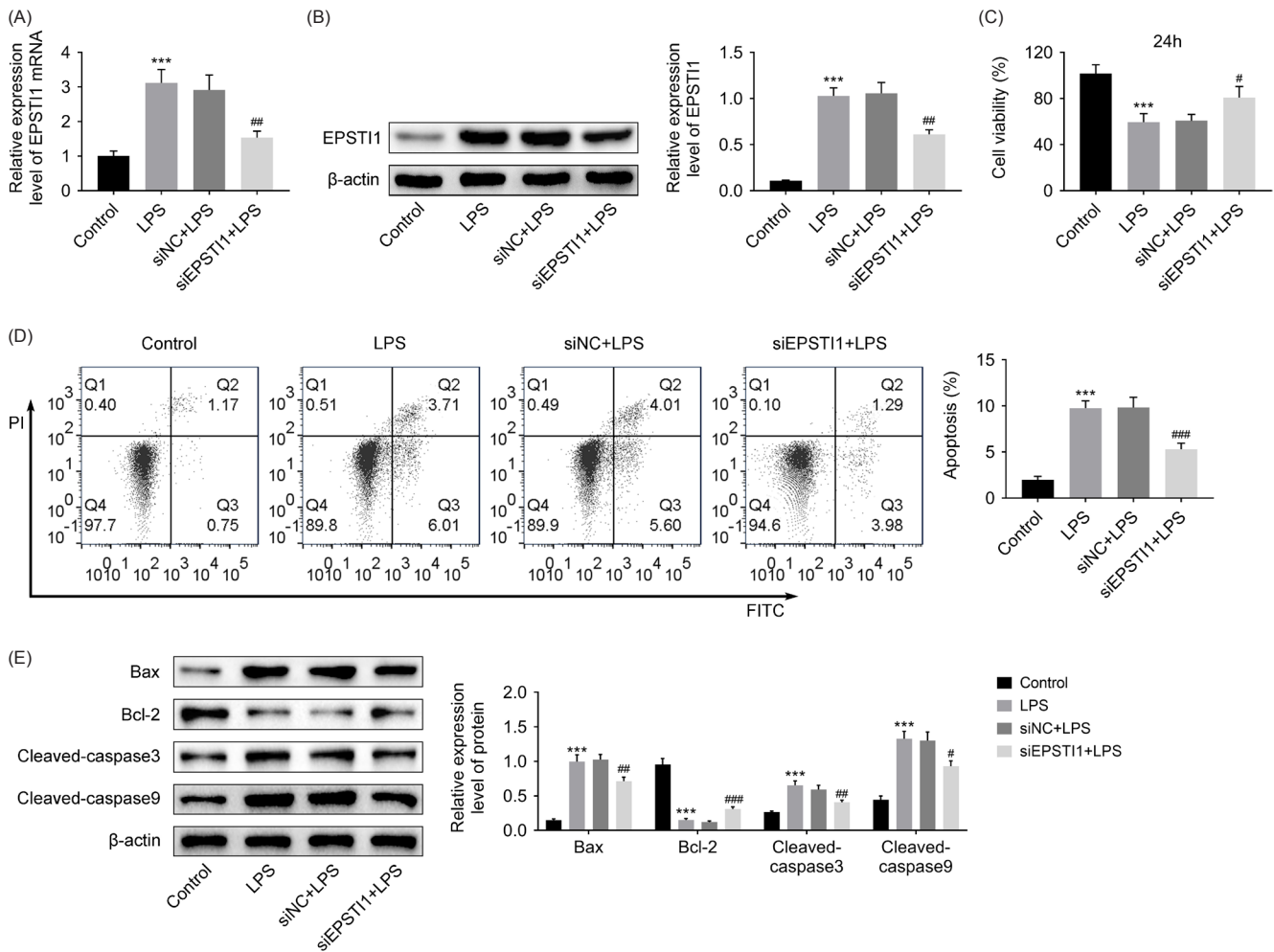


**Figure 2** Knockdown of EPSTI1 inhibited apoptosis after LPS treatment in WI-38 cells. (A) EPSTI1 expression was assessed by RT-qPCR after transfecting siEPSTI1 into LPS-treated (10  $\mu$ g/mL) WI-38 cells. (B) Protein level of EPSTI1 was determined by western blot analysis after transfecting siEPSTI1 into LPS-treated WI-38 cells. (C) Cell viability was assessed after transfecting siEPSTI1 into LPS-treated WI-38 cells. (D) Cell apoptosis was measured after transfecting siEPSTI1 into LPS-treated WI-38 cells. (E) Western blotting was implemented to determine the protein levels of Bax, Bcl-2, cleaved caspase 3, and cleaved caspase 9 after transfecting siEPSTI1 into LPS-treated WI-38 cells. \*\*\* $P < 0.001$  versus the control group. # $P < 0.05$ , ## $P < 0.01$ , and ### $P < 0.001$  versus the siNC+LPS group.

Similarly, immunoblotting displayed that siEPSTI1 visibly inhibited LPS-induced inflammatory responses as compared to the siNC group (Figure 3B). Collectively, knockdown of EPSTI1 suppressed inflammatory responses in LPS-treated WI-38 cells.

### Knockdown of EPSTI1 inactivated the NF- $\kappa$ B signaling pathway

Furthermore, proteins related to NF- $\kappa$ B signaling were quantified to investigate the mechanism underlying the regulatory effects of EPSTI1 on LPS-treated WI-38 cells. Figure 4 reveals that LPS remarkably elevated the ratios of p-p65/p65 and p-I $\kappa$ B $\alpha$ /I $\kappa$ B $\alpha$  as compared to the control ( $P < 0.001$ ). However, transfection with siEPSTI1 visibly reduced ratios of p-p65/p65 and p-I $\kappa$ B $\alpha$ /I $\kappa$ B $\alpha$  as compared to those

of siNC ( $P < 0.01$ ). Together, knockdown of EPSTI1 inactivated NF- $\kappa$ B signaling.

### Discussion

In the current study, EPSTI1 was highly expressed after being exposed to LPS, while cell viability was suppressed after LPS treatment. Knockdown of EPSTI1 repressed cell apoptosis and alleviated inflammatory responses in LPS-treated WI-38 cells. In addition, knockdown of EPSTI1 inactivated the NF- $\kappa$ B signaling pathway.

Pneumonia is a complex disorder caused by pathogenic microorganisms and manifests as local and systemic inflammatory responses. Specially, bacterial and viral co-infection is frequently observed in pediatric pneumonia.<sup>16</sup> LPS is a structure of Gram-negative bacteria, and accordingly,

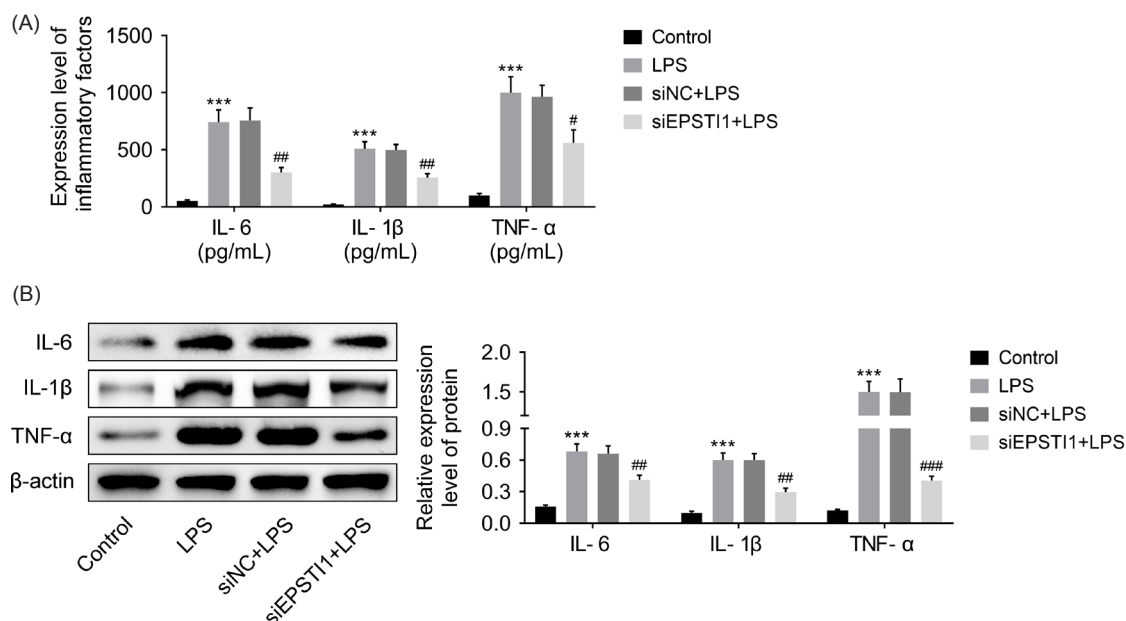


**Figure 3** Knockdown of EPST11 suppressed inflammatory responses in LPS-treated WI-38 cells. (A) ELISA was implemented to determine the levels of IL-6, IL-1 $\beta$ , and TNF- $\alpha$  after transfecting siEPST11 into LPS-treated WI-38 cells. (B) Protein levels of IL-6, IL-1 $\beta$ , and TNF- $\alpha$  were quantified by immunoblotting, followed by transfection of siEPST11 into LPS-treated WI-38 cells. \*\*\* $P < 0.001$  versus the control group. # $P < 0.05$ , ## $P < 0.01$ , and ### $P < 0.001$  versus the siNC+LPS group.

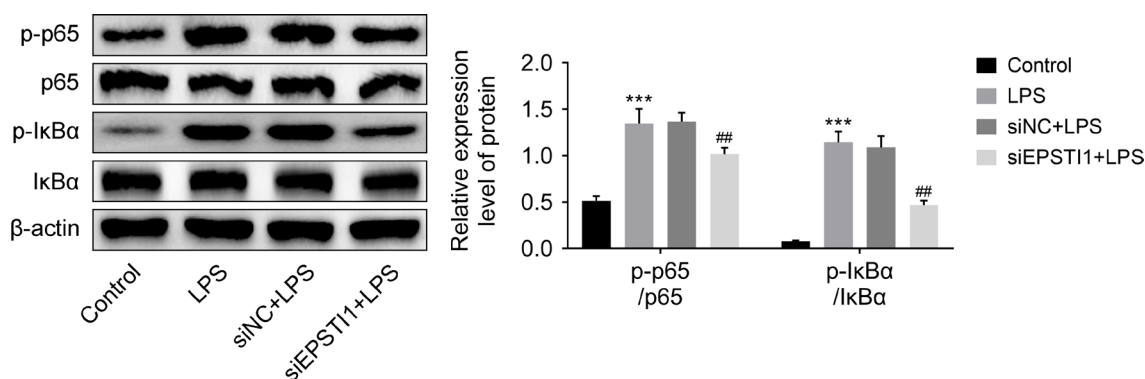


**Figure 4** Knockdown of EPST11 inactivated the NF- $\kappa$ B signaling pathway. Western blot analysis was employed to determine the protein levels of p-p65, p65, p-I $\kappa$ B $\alpha$ , and I $\kappa$ B $\alpha$ , and the ratios of p-p65/p65 and p-I $\kappa$ B $\alpha$ /I $\kappa$ B $\alpha$  were represented by histograms. \*\*\* $P < 0.001$  versus the control group. ## $P < 0.01$  versus the siNC+LPS group.

pneumonia caused by Gram-negative bacteria was modeled *in vitro*. Application of LPS can result in remarkable inflammatory reactions and apoptotic cells in WI-38 cells.<sup>17</sup> In this study, when LPS was administered into WI-38 cells, the apoptotic rate was increased while cell viability was significantly inhibited. Besides, the inflammatory products including IL-6, IL-1 $\beta$ , and TNF- $\alpha$  were upregulated. These findings implied that the cellular pneumonia model was induced successfully.

Elevated circulating proinflammatory products, including IL-6 and TNF- $\alpha$ , were observed in most patients with community-acquired pneumonia (CAP), and IL-6 concentration was associated with the severity.<sup>18</sup> It has been reported that the serum level of IL-6 was an independent factor for pneumococcal infection among children with CAP.<sup>19</sup>

Additionally, aberrant TNF- $\alpha$  has been shown to contribute to the development of lung cancer, COPD, or pneumonia, while elevated IL-6 concentration might be considered a potential biomarker for COPD progression.<sup>20</sup> Recently, IL-1 $\beta$  was highly expressed in endothelial cells of pulmonary tissues. Similarly, IL-6 and TNF- $\alpha$  both have significant immunoreactivities in COVID-19 specimen, suggesting that a cytokine storm might be triggered after infection.<sup>21</sup> A multicenter study demonstrated that for children with severe COVID-19, IL-1 $\beta$ , IL-6, and chemokine interferon-inducible protein-10 were dramatically increased, which could independently predict severe pneumonia in children with COVID-19.<sup>22</sup> In consistency with the above results, IL-6, IL-1 $\beta$ , and TNF- $\alpha$  were significantly upregulated in LPS-treated WI-38 cells, but knockdown of EPST11 obviously

suppressed inflammatory responses, indicating that IL-6, IL-18, and TNF- $\alpha$  contributed to the inflammatory responses while inhibiting EPST11 alleviated LPS-caused inflammation.

EPST11 gene is well-known as an important participant in cancer development and progression, as well as in some aspects of tumor immune interaction.<sup>23</sup> Interestingly, a previous study confirmed that EPST11 was implicated in the regulation of inflammatory responses in macrophages. The level of EPST11 was upregulated in LPS or interferon  $\gamma$ -treated macrophages, whereas knockdown of EPST11 provoked the differentiation of M2-type macrophages and polarization of M1 type. Besides, the silence of EPST11 could suppress proinflammatory products through inhibiting Stat1 and p65 nuclear localization and phosphorylation, which indicated that EPST11 might function as a regulator in the treatment of inflammatory disorders.<sup>24</sup> This study revealed that EPST11 was overexpressed after LPS stimuli, while knockdown of EPST11 attenuated the proinflammatory cytokines and inhibited apoptosis in WI-38 cells. These findings suggested that elevated EPST11 might be implicated in the development of pneumonia and provided a potentially important role of EPST11 in pneumonia.

Previous study has confirmed that EPST11 triggered NF- $\kappa$ B signaling and its nuclear translocation via interacting with valosin-containing protein (VCP) and inducing NF- $\kappa$ B inhibitor alpha degradation.<sup>10</sup> Meanwhile, the result also identified that EPST11 could inhibit cell apoptosis.<sup>10</sup> A recent study identified that EPST11 was increased in primary Sjögren's syndrome B cells, and it activated the NF- $\kappa$ B pathway and p-p65. However, inhibition of EPST11 dramatically decreased p-p65 expression and inactivated the NF- $\kappa$ B pathway.<sup>11</sup> Moreover, EPST11 promoted I $\kappa$ B $\alpha$  degradation and activated NF- $\kappa$ B signaling through interaction with VCP, whereas deficiency of EPST11 remarkably suppressed breast cancer cell invasion.<sup>25</sup> In the present study, LPS dramatically increased the ratios of p-p65/p65 and p-I $\kappa$ B $\alpha$ /I $\kappa$ B $\alpha$ , but knockdown of EPST11 significantly decreased these ratios. Collectively, knockdown of EPST11 inactivated NF- $\kappa$ B signaling.

In summary, the results identified that knockdown of EPST11 attenuated LPS-caused inflammatory injury in WI-38 cells through regulation of NF- $\kappa$ B signaling, which provided a potential target for the management of pneumonia at the cellular level.

## References

- Prina E, Ceccato A, Torres A. New aspects in the management of pneumonia. *Crit care*. 2016;20(1):1-9. <https://doi.org/10.1186/s13054-016-1442-y>
- Liu F, Wen Z, Wei J, Xue H, Chen Y, Gao W, et al. Epidemiology, microbiology and treatment implications in adult patients hospitalized with pneumonia in different regions of China: a retrospective study. *J Thorac Dis*. 2017;9(10):3875. <https://doi.org/10.21037/jtd.2017.09.18>
- Tramper-Stranders GA. Childhood community-acquired pneumonia: a review of etiology and antimicrobial treatment studies. *Paediatr Respir Res*. 2018;26:41-8. <https://doi.org/10.1016/j.prrv.2017.06.013>
- Nielsen HL, Rønnev-Jessen L, Villadsen R, Petersen OW. Identification of EPST11, a novel gene induced by epithelial-stromal interaction in human breast cancer. *Genomics*. 2002;79(5):703-10. <https://doi.org/10.1006/geno.2002.6755>
- Greenaway J, Moorehead R, Shaw P, Petrik J. Epithelial-stromal interaction increases cell proliferation, survival and tumorigenicity in a mouse model of human epithelial ovarian cancer. *Gynecol Oncol*. 2008;108(2):385-94. <https://doi.org/10.1016/j.ygyno.2007.10.035>
- Fan M, Arai M, Tawada A, Chiba T, Fukushima R, Uzawa K, et al. Contrasting functions of the epithelial-stromal interaction 1 gene, in human oral and lung squamous cell cancers. *Oncol Rep*. 2022;47(1):1-10. <https://doi.org/10.3892/or.2021.8216>
- Barclay WW, Woodruff RD, Hall MC, Cramer SD. A system for studying epithelial-stromal interactions reveals distinct inductive abilities of stromal cells from benign prostatic hyperplasia and prostate cancer. *Endocrinology*. 2005;146(1):13-8. <https://doi.org/10.1210/en.2004-1123>
- Fujino N, Ota C, Takahashi T, Suzuki T, Suzuki S, Yamada M, et al. Gene expression profiles of alveolar type II cells of chronic obstructive pulmonary disease: a case-control study. *BMJ Open*. 2012;2(6):e001553. <https://doi.org/10.1136/bmjopen-2012-001553>
- Shaath H, Vishnubalaji R, Elkord E, Alajez NM. Single-cell transcriptome analysis highlights a role for neutrophils and inflammatory macrophages in the pathogenesis of severe COVID-19. *Cells*. 2020;9(11):2374. <https://doi.org/10.3390/cells9112374>
- Gray J, Zhao J. Implications of epithelial-stromal interaction 1 in diseases associated with inflammatory signaling. *Cell Commun Insights*. 2016;(8). <https://doi.org/10.4137/CCI.S33397>
- Sun J-L, Zhang H-Z, Liu S-Y, Lian C-F, Chen Z-L, Shao T-H, et al. Elevated EPST11 promote B cell hyperactivation through NF- $\kappa$ B signalling in patients with primary Sjögren's syndrome. *Ann Rheum Dis*. 2020;79(4):518-24. <https://doi.org/10.1136/annrheumdis-2019-216428>
- Gasparini C, Feldmann M. NF- $\kappa$ B as a target for modulating inflammatory responses. *Curr Pharm Des*. 2012;18(35):5735-45. <https://doi.org/10.2174/138161212803530763>
- Dai J, Gu L, Su Y, Wang Q, Zhao Y, Chen X, et al. Inhibition of curcumin on influenza A virus infection and influenzal pneumonia via oxidative stress, TLR2/4, p38/JNK MAPK and NF- $\kappa$ B pathways. *Int Immunopharmacol*. 2018;54:177-87. <https://doi.org/10.1016/j.intimp.2017.11.009>
- Zhang L, Dong L, Tang Y, Li M, Zhang M. miR-146b protects against the inflammation injury in pediatric pneumonia through MyD88/NF- $\kappa$ B signaling pathway. *Infect Dis*. 2020;52(1):23-32. <https://doi.org/10.1080/23744235.2019.1671987>
- Livak KJ, Schmittgen TD. Analysis of relative gene expression data using real-time quantitative PCR and the 2- $\Delta\Delta$ CT method. *Methods*. 2001;25(4):402-8. <https://doi.org/10.1006/meth.2001.1262>
- Song Q, Xu B-P, Shen K-L. Effects of bacterial and viral co-infections of mycoplasma pneumoniae pneumonia in children: analysis report from Beijing Children's Hospital between 2010 and 2014. *Int J Clin Exp Med*. 2015;8(9):15666.
- Zhang Y, Zhu Y, Gao G, Zhou Z. Knockdown XIST alleviates LPS-induced WI-38 cell apoptosis and inflammation injury via targeting miR-370-3p/TLR4 in acute pneumonia. *Cell Biochem Funct*. 2019;37(5):348-58. <https://doi.org/10.1002/cbf.3392>
- Antunes G, Evans S, Lordan J, Frew A. Systemic cytokine levels in community-acquired pneumonia and their association with disease severity. *Eur Respir J*. 2002;20(4):990-5. <https://doi.org/10.1183/09031936.02.00295102>
- Vasconcellos ÁG, Cláudio J, Andrade D, Cardoso M-RA, Barral A, Nascimento-Carvalho CM. Systemic cytokines and chemokines on admission of children hospitalized with community-acquired pneumonia. *Cytokine*. 2018;107:1-8. <https://doi.org/10.1016/j.cyto.2017.11.005>
- Chen J, Li X, Huang C, Lin Y, Dai Q. Change of serum inflammatory cytokines levels in patients with chronic obstructive pulmonary disease, pneumonia and lung cancer. *Technol*

- Cancer Res Treat 2020;19:1533033820951807. <https://doi.org/10.1177/1533033820951807>
21. Frisoni P, Neri M, D'Errico S, Alfieri L, Bonuccelli D, Cingolani M, et al. Cytokine storm and histopathological findings in 60 cases of COVID-19-related death: from viral load research to immunohistochemical quantification of major players IL-1 $\beta$ , IL-6, IL-15 and TNF- $\alpha$ . Forensic Sci Med Pathol. 2022;18:4-19. <https://doi.org/10.1007/s12024-021-00414-9>
  22. Shafiek HK, El Lateef HMA, Boraey NF, Nashat M, Abd-Elrehim GA, Abouzeid H, et al. Cytokine profile in Egyptian children and adolescents with COVID-19 pneumonia: a multi-center study. Pediatr Pulmonol. 2021;56(12):3924-33. <https://doi.org/10.1002/ppul.25679>
  23. Zhang Y, Crawford HC, Pasca di Magliano M. Epithelial-stromal interactions in pancreatic cancer. Annu Rev Physiol. 2019;81:211-33. <https://doi.org/10.1146/annurev-physiol-020518-114515>
  24. Kim Y-H, Lee J-R, Hahn M-J. Regulation of inflammatory gene expression in macrophages by epithelial-stromal interaction 1 (Epsti1). Biochem Biophys Res Commun. 2018;496(2):778-83. <https://doi.org/10.1016/j.bbrc.2017.12.014>
  25. Li T, Lu H, Shen C, Lahiri SK, Wason MS, Mukherjee D, et al. Identification of epithelial stromal interaction 1 as a novel effector downstream of Krüppel-like factor 8 in breast cancer invasion and metastasis. Oncogene. 2014;33(39):4746-55. <https://doi.org/10.1038/onc.2013.415>